Performance Analysis of Full Duplex Wireless Network with Interference – A More Realistic Model

Georgino da Silva Baltazar
National Institute of Telecommunications - Inatel
Santa Rita do Sapucaí – Brazil
georginosilva@mtel.inatel.br

José Marcos C. Brito
National Institute of Telecommunications - Inatel
Santa Rita do Sapucaí – Brazil
brito@inatel.br

***Abstract*—In this paper, we propose an analytical Markovian model to analyze the performance of three operation modes in a linear wireless multi-hop network with interference. The study encompasses a comprehensive evaluation of both half and full-duplex operations, and the utilization of omnidirectional and directional antennas. Notably, our model incorporates the critical factor of buffering at network nodes. Several performance metrics were considered to evaluate the network performance: Block Probability, Capacity, Throughput, and Drop Probability. We show that in a system with a larger buffer size and high SNR, full-duplex performance is much better than half-duplex performance.**

Keywords: 6G; Full duplex communication; Performance analysis; Markovian models.

I. Introduction

The imminent global deployment of the fifth-generation network (5G) raises concerns about its ability to sustain the exponential growth in data traffic. As a result, researchers have been actively exploring the next wireless communication paradigm - the sixth generation (6G) [1][2]. Unlike its predecessor, 6G aims to revolutionize communication and integrate an unprecedented range of functionalities to enhance Quality of Service (QoS) and accommodate high traffic demands [3].

Extensive research has been conducted worldwide to meet the challenging requirements of 6G networks and the increasing demands of mobile data consumption. The goal is to improve existing networks and develop advanced and intelligent communication techniques that will transform 6G from an idea into reality. One of the most promising advancements in 6G is in-band full-duplex communication (IBFD), a technology that enables simultaneous data transmission and reception within the same frequency band [3][4]. The theoretical potential of IBFD communication is to double the spectral efficiency of the physical layer, optimizing resource sharing and meeting high spectral efficiency demands. However, this potential is impeded by the node's internal interference, also known as self-interference (SI), which arises when the node's transmitter interferes with its receiver [5][6].

Fortunately, recent research shows that SI can be reduced to acceptable levels, bringing IBFD communication closer to practical implementation [6]-[10]. However, there are still several important considerations for IBFD communication. Firstly, it necessitates the development of new radios capable of supporting this technology [10][11]. Secondly, the implementation of IBFD requires the design of new medium access control protocols and transmission modes [11]-[13].

In conclusion, as 5G paves the way for the future of wireless communication, the anticipation of 6G's emergence is driving intensive research to overcome challenges and create a network that surpasses all previous expectations. IBFD communication stands out as one of the key technologies with the potential to shape the landscape of 6G and bring about a new era of efficient and robust wireless connectivity.

Performance evaluation plays a crucial role in defining the optimal network configuration and mode of operation for IBFD wireless networks. Typically, IBFD communication is assessed through simulations [9]-[14]. However, in [15], the authors introduced a novel Markovian model to analyze the performance of IBFD technology in a multi-hop wireless network while considering interference. It is important to note that this model assumed the nodes in the network had no buffer. The findings in [15] revealed that the performance of the IBFD network is severely limited when nodes lack buffering capabilities. Consequently, a more comprehensive modeling approach that considers buffers in the nodes is necessary to gain a deeper understanding of the actual benefits of the IBFD network and its optimal configurations.

This paper proposes an advanced Markovian model that enables a comprehensive performance analysis of IBFD technology in wireless networks (including half-duplex networks). Additionally, we consider both omnidirectional and directional antennas while accounting for the extent of interference reaching the last node of the network. The novelty in this model is that it incorporates the presence of buffers in the nodes, resulting in a more realistic model than the one presented in [15]. The performance metrics utilized are consistent with those presented in [15]: Block Probability, Capacity, Throughput, and Drop Probability.

The remainder of this paper is structured as follows: Section II outlines the adopted network scenario; Section III introduces the proposed Markovian model; Section IV describes and calculates the performance metrics; Section V presents the numerical results; and finally, in Section VI, we provide the conclusion.

II. NETWORK SCENARIO AND ASSUMPTIONS

This paper uses the network configuration introduced in [15], representing a wireless multi-hop network with one-way traffic. The network comprises four nodes: S (Source), 1, 2, and D (Destination). The Source (S) transmission is relayed through intermediate nodes 1 and 2 to reach the Destination (D). However, it is essential to consider that the transmissions from node S to node 1 also propagate as interference signals, reaching nodes 2 and D simultaneously, as depicted in Figure 1. Likewise, the transmission from node 1 to node 2 also acts as an interference signal, reaching node D. This interference phenomenon is a crucial aspect that warrants careful analysis in our study.

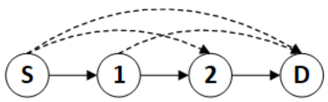

Figure 1. Network scenario.

Following the work presented in [12], network nodes can be configured using two parameters: the communication type, which can be either Half Duplex (HD) or Full Duplex (FD), and the antenna type, which can be either Directional Antennas (DA) or Omnidirectional Antennas (ODA). Nodes operating in Half Duplex (HD) mode can only transmit or receive data at any given time, while Full-Duplex (FD) nodes can simultaneously transmit and receive data.

In this paper, we focus on the study of three types of nodes:

1) A[Full, Omni]: This type of node is equipped with Full-Duplex (FD) transmission technology and features two Omnidirectional Antennas (ODA): one for transmitting and one for receiving.

2) B[Half, Direc]: This node type utilizes Half Duplex (HD) transmission technology and is equipped with three antennas: one Omnidirectional Antenna (ODA) for reception and two Directional Antennas (DA) for transmission. Although data transmission occurs in only one direction, the additional transmitting antenna can be used for control information transmission, which is not considered in the modeling.

3) C[Full, Direc]: Similar to B[Half, Direc], this node type also has three antennas, but it operates with Full-Duplex (FD) transmission technology. The setup includes one Omnidirectional Antenna (ODA) for reception and two Directional Antennas (DA) for transmission.

The analysis considers that all nodes in the network operate in a single mode: Mode A[Full, Omni], Mode B[Half, Direc], or Mode C[Full, Direc]. Figure 2 illustrates the operation of each mode.

In mode A[Full, Omni], nodes S and 1 or nodes 1 and 2 can transmit simultaneously but with different departure rates. Two steps are required to complete a transmission in the network: (i) transmission from S to 1 with rate of μ_1 and transmission from 1 to 2 with rate of μ_2 with interference from S, resulting in $\mu_2 < \mu_1$; (ii) Node 2 transmits data to D with a rate of μ_1 when it is the only node transmitting. However, if node 1 is also transmitting simultaneously with node 2, D experiences interference from node 1, causing the transmission rate to be μ_2 from 2 to D.

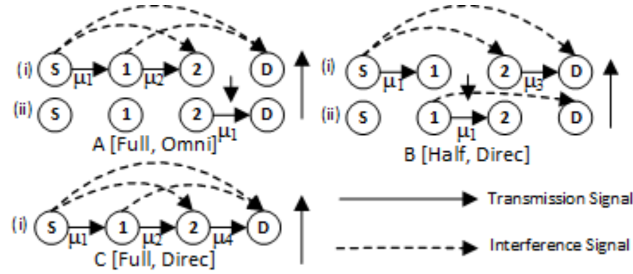

Fig 2. Operation process for each operation mode [16].

In mode B [Half, Direc], the transmission process involves two steps: (i) transmission from S to 1 occurs at a rate of μ_1, and simultaneously, there is a transmission from 2 to D with rate μ_3. Due to the interference caused by S on D, the transmission rate μ_3 is lower than μ_1; (ii) after the first step, node 1 transmits data to node 2 at a rate of μ_1. Directional antennas are utilized in this mode, allowing nodes S and 2 to transmit simultaneously. However, none can transmit and receive simultaneously because all nodes are half-duplex.

In the mode C[Full, Direc], only one step is necessary to complete a transmission: (i) transmission from S to 1 with rate μ_1, from 1 to 2 with rate $\mu_2 < \mu_1$, and from 2 to D with rate $\mu_4 < \mu_2$. μ_4 is the lowest rate among all rates because node D is experiencing double interference from S and 1. Here, all nodes can transmit and receive simultaneously because the nodes are FD and use Directional antennas. However, when S and 2 are transmitting simultaneously, 2 transmits to D at a rate of μ_3.

III. MARKOVIAN MODEL

In this session, we propose a multidimensional Continuous Time Markovian model to represent the various operation modes of the network. The model encompasses transitions due to packet arrivals and departures within the network and packet transmissions from one node to another.

The arrival process follows a Poisson distribution with an average arrival rate of λ packets/second. On the other hand, the service time follows an exponential distribution with a mean value of $1/\mu_1$, resulting in a service rate of μ_1 packets/second in the absence of interference. However, this rate can vary based on the interference experienced at the receiver, as illustrated in Figure 2.

Figure 3 illustrates the state diagram for mode B [Half, Direc], where the buffer size is set to 1 (actually, we consider buffer size equal to 5 and 10 in our analysis). This modeling approach is consistent with the methodology used for other modes, enabling us to compute the desired metrics efficiently.

In our analysis, we adopt a state representation for the Markov chains as follows: $x = \{i(wi), j(wj), k(wk)\}$, where: *i* represents the presence or absence of transmission from node S to node 1; *wi* represents the number of packets waiting at node S; *j* represents the presence or absence of transmission from node 1 to node 2; *wj* represents the number of packets waiting at node 1; *k* represents the presence or absence of transmission from node 2 to node D; *wk* represents the number of packets waiting at node 2. This state representation enables us to model and analyze the various possible configurations of the network, considering the existence of transmissions and the queue lengths at each node. Using this multidimensional representation, we can accurately characterize the system's behavior and calculate relevant performance metrics for different operation modes.

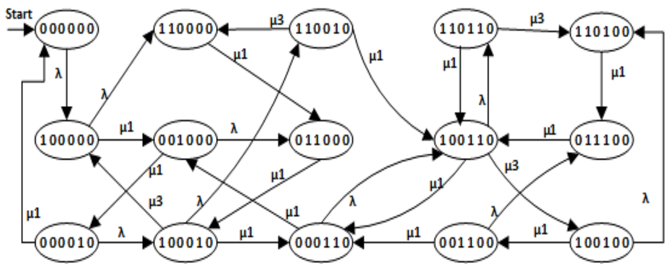

Fig 3. State diagram - Mode B[Half, Direc] with b = 1.

The subset {hop, node} will be described as a server to simplify the notation. Thus, $\{i(wi)\}$ is defined as server i, $\{j(wj)\}$ is defined as server j, and $\{k(wk)\}$ is defined as server k. For example, $x = \{1(1),1(0),0(0)\}$ represents a state where server i has one packet in the buffer and is transmitting simultaneously with server k, as we can see in Figure 3; in this state, server i is transmitting with a rate μ_1 and server k is transmitting with a rate μ_3. μ_1 represents the departure rate in the absence of interference, μ_2, μ_3 and μ_4 represent the departure rates in the presence of interference. The derivations of the mathematical expressions for these rates are presented below.

Using Shannon's Channel Capacity Theorem, considering B = 1 Hz for normalization purposes, we determined the channel capacity expression for each link:

$$\Phi = \log_2(1 + SNR). \tag{1}$$

Where Φ is a given link's channel capacity, and SNR is that link's signal-to-noise ratio.

In the absence of interference, when a node transmits with rate μ_1, the SNR is given by:

$$SNR_1 = \frac{\frac{Pt*Gt*Gr}{L}}{N}. \tag{2}$$

Where Pt is the transmit power, Gt and Gr are the gains of transmission and reception antennas, respectively, L is the free space attenuation, and N is the power noise. Let us assume that adding Equation 2 into Equation 1 results in the departure rate of μ_1. Then, the capacity of the channel without interference for a given link is computed by:

$$\Phi_1 = \log_2(1 + SNR_1) = \mu_1. \tag{3}$$

To compute the SNR_2, SNR_3, and SNR_4 in the presence of interference, we consider that the nodes are equidistant, and the attenuation in free space is proportional to the square of the distance.

Thus, the SNR for a link where the node transmits with departure rate of μ_2 is computed by:

$$SRN_2 = \frac{4*SNR_1}{4+SNR_1}. \tag{4}$$

The SNR for a link with departure rate μ_3 is calculated by:

$$SRN_3 = \frac{9*SNR_1}{9+SNR_1}. \tag{5}$$

Finally, for a link where the departure rate is μ_4, the SNR is:

$$SRN_4 = \frac{144*SNR_1}{144+36*SNR_1+16*SNR_1}. \tag{6}$$

Using the relations given by equations 4, 5, and 6 and Equation 3, we can calculate the departure rates μ_2, μ_3, and μ_4 for a given departure rate of μ_1.

We must define all possible state transitions for all modes to analyze the system. Table I illustrates the transitions for Model A[Full, Omni], where _PA represents the arrival of a packet and _TX_*a*-*b* represents the transmission from server *a* to *b*. A similar table can be defined for the other modes.

The stationary probabilities $\pi(x)$ can be calculated using the global equilibrium equations and the normalization equation represented by:

$$\pi Q = 0, \sum_{x \epsilon S} \pi(x) = 1, \tag{7}$$

where π represents the vector of stationary probabilities, Q is the transition rate matrix, and S is the set of all possible states. S and Q can be constructed using the transition patterns in Table I for Mode A[Full, Omni]. A similar approach can be performed for Mode B[Half, Direct] and Mode C[Full, Direct].

After determining the departure rates considering interference and stationary probabilities, using (7), we can evaluate the system performance for different metrics. The following section presents the derivations of the mathematical expressions for these metrics.

Table I.Transition Equations for Model A[Full, Omni]

$$S = \{x | 0 \le i, wi, j, k, wk \le 1; i + j + k \le 2; i + k \le 1; i + wi \le 1; k + wk \le 1; wj = 0;\}$$

Event	Destination state	Rate	Condition
1_PA	$i + 1$	λ	$i = wi = j = wj = k = wk = 0$
2_PA	$wi + 1$	λ	$i = 1; wi < b; j \le 1; wj \le b; k = 0; wk \le b$
3_PA	$wi + 1$	λ	$i = 0; wi < b; j \le 1; wj \le b; k = 1; wk \le b$
4_TX_i-j	$i - 1, j + 1$	μ_1	$i = 1; wi = j = wj = k = wk = 0$
5_TX_i-j	$wi - 1, j + 1$	μ_1	$i = 1; wi > 0; j = wj = k = wk = 0$
6_TX_i-j	$i - 1, wj + 1$	μ_1	$i = 1; wi = 0; j = 1; wj < b; k = wk = 0$
7_TX_i-j	$wi - 1, wj + 1$	μ_1	$i = 1; wi > 0; j = 1; wj < b; k = wk = 0$
8_TX_i-j	$i - 1, j + 1, k + 1, wk - 1$	μ_1	$i = 1; wi \le b; j = wj = k = 0; wk > 0$
9_TX_i-j	$i - 1, j + 1, k + 1, wk - 1$	μ_1	$i = 1; wi \le b; j = 1; wj < b; k = 0; wk > 0$
10_TX_i-j	$i - 1$ dropped	μ_1	$i = 1; wi = 0; j = 1; wj = b; k = wk = 0$

11_TX_j-k	$wi-1$ dropped	μ_1	$i=1; wi>0; j=1; wj=b; k=wk=0$
12_TX_i-j	$i-1, k+1, wk-1$ dropped	μ_1	$i=1; wi>0; j=1; wj=b; k=0; wk>0$
13_TX_j-k	$j-1, k+1$	μ_1	$i=wi=0; j=1; wj=k=wk=0$
14_TX_j-k	$j-1, wk+1$	μ_2	$i=1; wi\leq b; j=1; wj=k=0; wk<b$
15_TX_j-k	$j-1, wk+1$	μ_1	$i=0; wi\leq b; j=1; wj=0; k=1; wk<b$
16_TX_j-k	$wj-1, k+1$	μ_1	$i=wi=0; j=1; wj>0; k=wk=0$
17_TX_j-k	$wj-1, wk+1$	μ_2	$i=1; wi\leq b; j=1; wj>0; k=0; wk<b$
18_TX_j-k	$wj-1, wk+1$	μ_1	$i=0; wi\leq b; j=1; wj>0; k=1; wk<b$
19_TX_j-k	$j-1$ dropped	μ_2	$i=1; wi\leq b; j=1; wj=k=0; wk=b$
20_TX_j-k	$j-1$ dropped	μ_1	$i=0; wi\leq b; j=1; wj=0; k=1; wk=b$
21_TX_j-k	$wj-1$ dropped	μ_2	$i=1; wi\leq b; j=1; wj>0; k=0; wk=b$
22_TX_j-k	$wj-1$ dropped	μ_1	$i=0; wi\leq b; j=1; wj>0; k=1; wk=b$
23_TX_k-d	$k-1$	μ_2	$i=wi=0; j=1; wj\leq b; k=1; wk=0$
24_TX_k-d	$k-1$	μ_1	$i=wi=0; j=0; wj\leq b; k=1; wk=0$
25_TX_k-d	$i+1, wi-1, k-1$	μ_2	$i=0; wi>0; j=1; wj\leq b; k=1; wk\leq b$
26_TX_k-d	$i+1, wi-1, k-1$	μ_1	$i=0; wi>0; j=0; wj\leq b; k=1; wk\leq b$
27_TX_k-d	$wk-1$	μ_2	$i=wi=0; j=1; wj\leq b; k=1; wk>0$
28_TX_k-d	$wk-1$	μ_1	$i=wi=0; j=0; wj\leq b; k=1; wk>0$

IV. Performance Metrics

To analyze the system's performance we consider the following metrics: blocking probability, drop probability, system capacity, throughput, and the average number of elements in the system.

The blocking probability, P, represents the sum of the probabilities of the states where the buffer of the server *i* is at its total capacity, leading to a scenario where the server *i* can accept no new packets:

$$P = \sum_{x\in S} \pi(x),\ if\ wi = b, \quad (8)$$

where *b* is the buffer capacity of server *i*.

The system capacity, C, defines the average number of successful transmissions per unit time and is calculated by:

$$C = \sum_{x\in S} \pi(x)\,\gamma, \quad (9)$$

where $\gamma = \begin{cases} \mu_{1,}\ if & k=1 \\ \mu_2, if & j=1\ and\ k=1 \\ \mu_3,\ if & i=1\ and\ k=1 \\ \mu_4,\ if & i=1,\ j=1\ and\ k=1 \end{cases}$

$k=1$ means that in this state server k is transmitting to the destination, and μ_1, μ_2, μ_3, and μ_4 represent the possible departure rates at the server *k*.

The drop probability, D, represents the probability that a packet that entered the network will be discarded before reaching its destination and is computed by:

$$D = 1 - ST, \quad (10)$$

where ST is the probability that a packet that entered the network is successfully transmitted to the destination, calculated by the ratio of the average rate of packets successfully transmitted, represented by C, to the average rate of packets entering the network, given by the Equation 11,

$$ST = C/\lambda(1-P), \quad (11)$$

where, C is the system capacity, given by Equation (9), and $\lambda(1-P)$ represents the average number of packets entering the network.

The Throughput is defined as the system capacity divided by the total packets arrival rate: $Th = C/\lambda$ (12).

V. Numerical Results

This section presents some numerical results for the three modes described in Section II. The calculations were performed using Matlab with the following parameters settings: arrival rate (λ), variyng from 1 to 10 pac/s; departure rate μ_1, set to 10 pac/s; departure rates considering the existence of interference ($\mu_{2,}$ μ_3 , and μ_4), calculated as explained in Section III, using equations 3, 4, 5 and 6; SNR without interference (SNR_1), considered values of 10, 50, and 100. The analysis has been conducted considering two buffer scenarios: one with a buffer size of 5 and another with a buffer size equal to 10. This approach allows for a comprehensive assessment of how the buffer size impacts the system's performance.

Figures 4 and 5 show the blocking probability. In the case of Mode A[Full,Omni], the blocking probability remains unaffected by buffer size when the buffer is equal to or greater than 5. However, for Modes B[Half, Direc] and C[Full, Direc], the blocking probability exhibits a downward trend as the buffer size increases. Specifically, Mode C[Full, Direc] exhibits the lowest blocking probability, followed by Mode B[Half, Direc], while Mode A[Full,Omni] displays the highest blocking probability across all buffer sizes.

Furthermore, a clear correlation emerges: higher SNR values correspond to lower blocking probabilities, indicating that elevated SNR levels contribute to improved overall system performance.

Figures 6 and 7 show the System Capacity, and figures 8 and 9 show the Throughput. Notably, mode C[Full, Direc] emerges as the frontrunner in terms of both System Capacity and Throughput, showcasing superior performance compared to modes A[Full, Omni] and B[Half, Direc]. It can also be seen that the performance of modes A[Full, Omni] and B[Half, Direc] is almost equal for buffers greater than or equal to 5. The performance of mode C[Full, Direc] improves dramatically as the buffer increases. Mode B[Half, Direc] with SNR_1 =10 has the worst performance.

Finally, the Drop Probability is shown in figures 10 and 11. The Drop Probability is almost zero for mode A[Full, Omni] with a buffer equal to 10. In modes B[Half, Direc] and C[Full, Direc], the drop probability decreases with the buffer length increases. One can also see that mode B[Half, Direc] has a higher blocking probability.

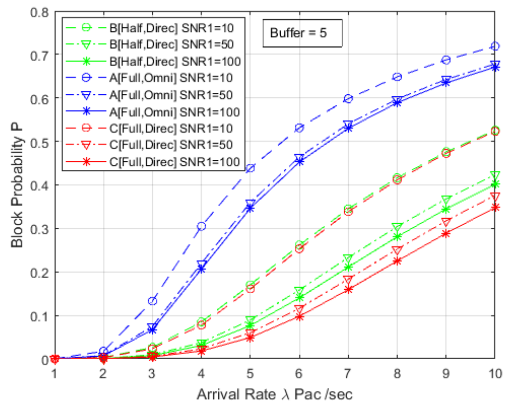

Fig 4. *Blocking Probability* with buffer = 5

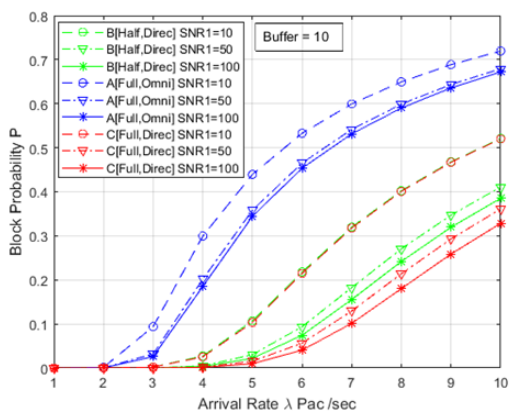

Fig 5. Blocking Probability with buffer = 10

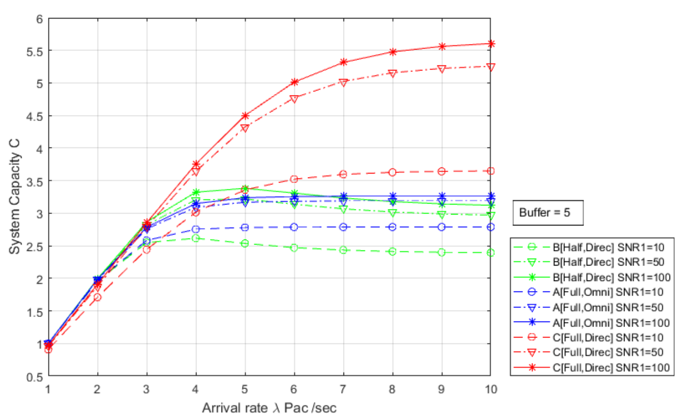

Fig 6. System Capacity with buffer equal to 5

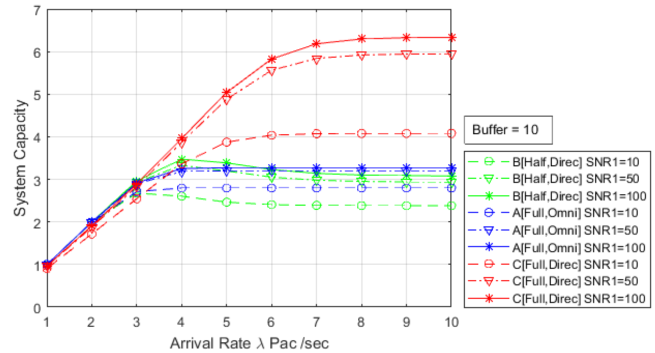

Fig 7. System Capacity with buffer equal to 10

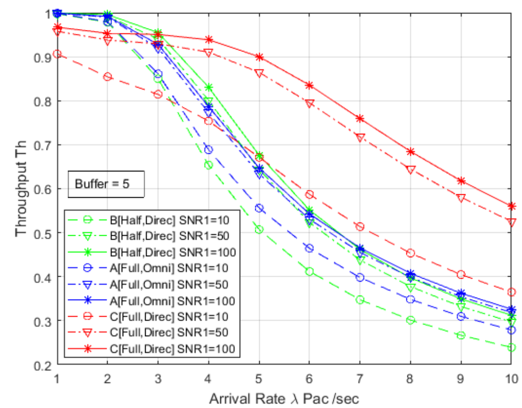

Fig 8. System Throughput with buffer equal to 5

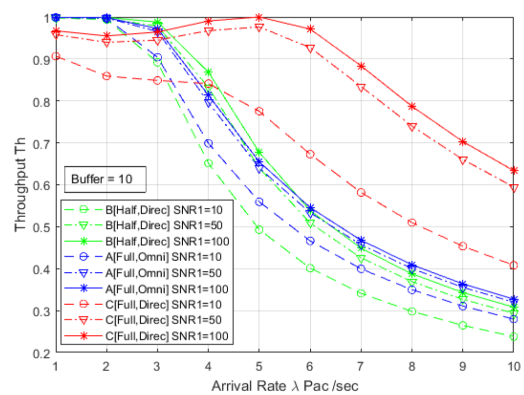

Fig 9. System Throughput with buffer equal to 10.

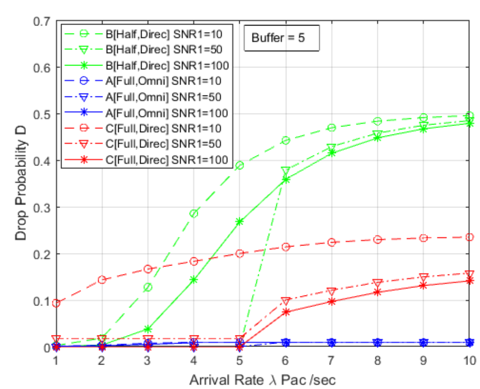

Fig 10. Drop Probability with buffer equal to 5.

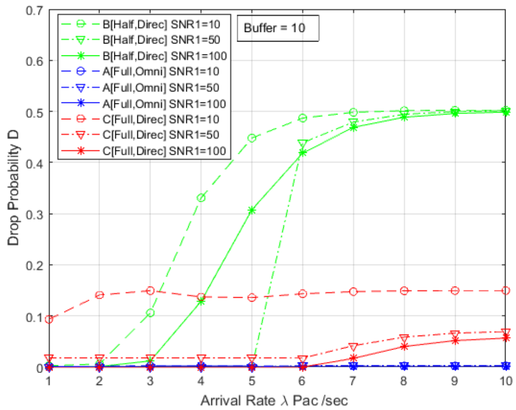

Fig 11. Drop Probability with buffer equal to 10.

VI. CONCLUSION

This paper introduces an innovative analytical Markovian model designed to assess the performance of three distinct operational modes within a linear wireless multi-hop network. This comprehensive analysis considers potential interference scenarios, encompassing both half and full-duplex operations and the utilization of omnidirectional and directional antennas. Notably, our model incorporates the crucial consideration of buffering at network nodes.

Our findings yield compelling insights. Mode C[Full,Direc], characterized by a combination of full-duplex operation, directional antennas, SNR=100, and a buffer capacity of 10 positions, emerges as the mode that exhibits optimal performance across multiple metrics. This encompasses enhanced capacity, increased throughput, and minimized blocking probability.

Conversely, our investigation highlights mode B[Half,Direc] with SNR=10 and a buffer size of 5 positions as the mode with the least favorable performance characteristics. This underscores the significance of effective buffering and operational configurations in influencing overall performance outcomes.

In a broader context, our results underscore the advantages of leveraging a larger buffer size, particularly in conjunction with full-duplex operations and omnidirectional/directional antennas. This combination stands out as a robust choice, demonstrating superior performance compared to utilizing half-duplex operations with directional antennas.

In summary, our analytical model facilitates a comprehensive evaluation of operational modes in a wireless multi-hop network, shedding light on the performance dynamics and offering valuable guidance for designing efficient and effective network configurations.

ACKNOWLEDGMENT

This work was partially supported by RNP, with resources from MCTIC, Grant No. 01245.020548/2021-07, under the Brazil 6G project of the Radiocommunication Reference Center (Centro de Referência em Radiocomunicações - CRR) of the National Institute of Telecommunications (Instituto Nacional de Telecomunicações - Inatel), Brazil, and by Huawei, under the project Advanced Academic Education in Telecommunications Networks and Systems, contract No PPA6001BRA23032110257684

REFERENCES

[1] M. Giordani, M. Polese, M. Mezzavilla, S. Rangan and M. Zorzi, “Toward 6G Networks: Use Cases and Technologies”, in IEEE Communications Magazine, vol. 58, no. 3, pp. 55-61, March 2020.

[2] 6G Flagship Project, “Key Drivers and Research Challenges for 6G Ubiquitous Wireless Intelligence”, University of Oulu, September 2019.

[3] Zhao, Y., Zhao, J., Zhai, W., Sun, S., Niyato, D., Lam, “A Survey of 6G Wireless Communications: Emerging Technologies” , In: Arai, K. (eds) Advances in Information and Communication. FICC 2021. Advances in Intelligent Systems and Computing, vol 1363. Springer, Cham.

[4] S. Chen, Y.-C. Liang, S. Sun, S. Kang, W. Cheng, and M. Peng, “A Survey on Green 6G Network: Architecture and Technologies”, IEEE Access, vol. 7, pp. 175 758–175 768, 2019.

[5] K. Eshteiwi, G. Kaddoum, B. Selim, and F. Gagnon,“ Impact of co-channel interference and vehicles as obstacles on full-duplex v2v cooperative wireless network” IEEE Trans. Veh. Technol., pp. 1–1, May 2020.

[6] Muhammad Sohaib Amjad and Ozgur Gurbuz, “Linear Digital Cancellation with Reduced Computational Complexity for Full-Duplex Radios”, IEEE Wireless Communications and Networking Conference (WCNC) 2017.

[7] Elsayed Ahmed and Ahmed M. Eltawil, “All-Digital Self-interference Cancellation Technique for Full-duplex Systems”, IEEE Transactions on Wireless Communications 2015.

[8] Muhammad Sohaib Amjad and Ozgur Gurbuz, “Linear Digital Cancellation with Reduced Computational Complexity for Full-Duplex Radios”, IEEE Wireless Communications and Networking Conference (WCNC) 2017.

[9] Xiaojing Huang and Y. Jay Guo. “Radio Frequency Self-interference Cancellation With Analog Least Mean-Square Loop”, IEEE Transactions on Microwave Theory and Techniques. 2017.

[10] Min Soo Sim; MinKeun Chung; Dongkyu Kim; Jaehoon Chung; Dong Ku Kim; Chan-Byoung Che, “Nonlinear Self-Interference Cancellation for Full-Dplex Radios: From Link-Level and System-Level Performance Perspectives”, IEEE Communications Magazine 2017.

[11]] Ken Miura and Masaki Bandai. “Node architecture and MAC protocol for full duplex wire-less and directional antennas”, In Personal Indoor and Mobile Radio Communications (PIMRC), 23rd International Symposium on, pages 369–374. IEEE, 2012

[12] Sanjay Goyal, Pei Liu, Ozgur Gurbuz, Elza Erkip, and Shivendra Panwar. “A distributed MAC protocol for full duplex radio”, In Signals, Systems and Computers, 2013 Asilomar Con-ference on, pages 788–792. IEEE, 2013.

[13] Kenta Tamaki, H Ari Raptino, Yusuke Sugiyama, Masaki Bandai, Shunsuke Saruwatari, Takashi Watanabe, et al. “Full duplex media access control for wireless multi-hop networks”, In VTC Spring, pages 1–5, 2013.

[14] Karaputugala Madushan Thilina, Hina Tabassum, Ekram Hossain, and Dong In Kim. Medium access control design for full duplex wireless systems: challenges and approaches. IEEE Communications Magazine, 53(5):112–120, 2015.

[15] G. D. S. Baltazar and J. M. C. Brito, "Modeling and Analysis of Full Duplex Wireless Systems with Interference," 2022 13th International Conference on Information and Communication Systems (ICICS), Irbid, Jordan, 2022, pp. 479-484.